Journal of Alloys and Compounds 509 (2011) 5105–5111

Contents lists available at ScienceDirect

Journal of Alloys and Compounds

journal homepage: www.elsevier.com/locate/jallcom

Electrical characteristics of Au/Pyronine-B/moderately doped n-type InP Schottky structures in a wide temperature range

M. Soylu [a,*], B. Abay [b], Y. Onganer [c]

[a] Department of Physics, Faculty of Sciences, University of Bingol, Bingol, Turkey
[b] Department of Physics, Faculty of Sciences, Ataturk University, Erzurum, Turkey
[c] Department of Chemistry, Faculty of Sciences, Ataturk University, Erzurum, Turkey

ARTICLE INFO

Article history:
Received 5 January 2010
Received in revised form 26 January 2011
Accepted 27 January 2011
Available online 1 March 2011

Keywords:
InP
Schottky diode
Pyronine-B
Gauss distribution

ABSTRACT

The temperature dependence of current–voltage (I–V) characteristics of the Au/Pyronine-B/moderately doped (MD) n-InP Schottky barrier diode has been systematically investigated in the temperature range of 160–400 K. Modification of the interfacial potential barrier for metal/InP diodes has been achieved using a thin interlayer of the pyronine B organic semiconductor. It has been observed that ideality factor n (=1.10) remained close to ideal limit while barrier height of Au/Pyronine-B/n-InP structure increased about 0.180 eV with respect to Au/n-InP in the previous study, at room temperature. The forward I–V characteristics have been interpreted on the basis of standard thermionic emission (TE) theory and assumption of a Gaussian distribution of the barrier height. The apparent barrier height and the ideality factor derived by using thermionic emission theory have been found to be strongly temperature dependent. That is, it has been understood that the ideality factor decreases while the apparent barrier height (Φ_{b0}^{j}) increases with increasing temperature. It has been shown that the conventional $\ln(J_0/T^2)$ vs. $1000/T$ plot exhibits a non-linearity below 240 K. It has been demonstrated that this behaviour results due to the barrier height inhomogeneities prevailing at the metal–semiconductor interface. The mean barrier height ($\overline{\Phi}_{b}^{j}$) and the Richardson constant (A^*) values were obtained as 0.961 eV and 17.73 A K^{-2} cm^{-2}, respectively, by means of the modified Richardson plot, $[\ln(J_0/T^2) - (q^2\sigma_0^2/2k^2T^2)]$ vs. $1/T$. The value of Richardson constant A^* obtained from this plot is close to the theoretical value of 9.4 A K^{-2} cm^{-2} for n-InP. As a result, it can be concluded that the temperature dependent characteristic parameters for Au/Pyronine-B/MD n-InP structure can be succesfully explained on the basis of TE mechanism with Gaussian distribution of the barrier height.

© 2011 Elsevier B.V. All rights reserved.

1. Introduction

The metal–semiconductor (MS) structures are of important for applications in the electronic industry. The popularity of such studies, which is rooted in their importance to the semiconductor industry, does not assure uniformity of the results or of the interpretation. For that reason, there is a vast number of reports of experimental studies of metal/semiconductor systems. These applications consist of microwave field effect transistors, radio-frequency detectors, phototransistors, heterojunction bipolar transistors, quantum confinement devices and space solar cell [1]. The performance and reliability of a Schottky contact are highly influenced by the interface quality between the deposited metal and the semiconductor surface. Due to the stability of nonpolymeric organic compounds, they have been employed particularly in electronic devices for more than the last two decades [2–5]. It has been observed recently that both conductive polymers (CP) and charge transfer organic complexes can be used to obtain rectifiying junctions with metal and inorganic semiconductors [6,7]. Lately, the use of thin organic interlayers in metal/inorganic semiconductor junctions is a promising direction for applications in high-frequency microwave technology [8,9]. Furthermore, many studies have been recently made for the barrier height (BH) enhancement or modification using the thin organic interfacial layers [10–18]. The resulting junction, which involves a hybrid structure between the p and n junction and the Schottky diode has been called pseudo-Schottky diode [19]. Hence, at the present time, the main technological issue in the study of semiconductor interface is the continious control of the BH of high quality SBDs with low departure of ideality factor (n) from unity.

In order to understand the conduction mechanism of the Schottky barrier diode (SBD), many attempts have been made. The analysis of the current–voltage (I–V) characteristics of Schottky barriers on the basis of thermionic emission diffusion (TED) the-

* Corresponding author. Tel.: +90 426 213 2550; fax: +90 426 213 2866.
E-mail address: soylum74@yahoo.com (M. Soylu).

0925-8388/$ – see front matter © 2011 Elsevier B.V. All rights reserved.
doi:10.1016/j.jallcom.2011.01.183

ory reveals an abnormal decrease of the barrier height (BH) and increase of the ideality factor with decreasing temperature [20–24]. Explanation of the possible origin of such anomalies has been proposed by taking into account the interface state density distribution [25], quantum-mechanical tunnelling [1,26,27], image force lowering [1] and most recently the lateral distribution of BH inhomogeneities [28,29]. In addition, a Gaussian distribution of the BH over the contact area has been assumed to describe the inhomogeneities as an other way too [30].

A significant increase in the ideality factor and decrease in the SBH at low temperature are possibly originated by structural defects in the semiconductor, inhomogeneous doping, interface roughness, interfacial reactions, diffusion/interdiffusion of the contaminations of applied materials on semiconductor surface, inhomogeneities of thickness and composition of the layer, and non-uniformity of interfacial charges or the presence of a thin insulating layer between the metal and the semiconductor [31].

Semiconducting organic materials can be used in different condensed matter physics applications, such as organic light emitting diodes, organic field effect transistors, Schottky diodes, photovoltaic (PV) and solar cells, organic spintronics and so on. Furthermore, more recently, electronic systems are moving to the ultimate scale of molecular entities, as demonstrated by the growing interest in understanding transport through organic molecules bridging two metal contacts. Organic light-emitting diodes (OLED) have been investigated intensively [32–35] due to their promising applications in large-area, flat and ultra thin displays. Up to now, fluorescence based organic electroluminescent devices have reached the commercial level. In the future, OLED displays have the potential to be brighter than a conventional TV screen with much higher efficiency, brilliant colors, large viewing angle, switching times fast enough for video frequency and lifetimes well above 10,000 h. Organic-on-inorganic heterostructure diodes based on crystalline thin films of the organic materials PTCDA (3,4,9,10-perylenetetracarboxylic dianhydride) and CuPc (copper phtalocyanine) deposited on n-type InP were investigated by Urbach et al. [20]. Recently, Sharma et al. [21] have studied the *I–V* characteristics in dark as well as under illumination and *C–V* characteristics in dark of the sandwich devices having ITO/pyronine-G(Y)/Al and ITO/pyronine-G(Y)/In prepared by the spin coating technique. But, the effect of Pyromine-B film on the barrier height enhancement of Au/InP structure has not been studied yet.

Indium phosphide (InP) being one of the III–V compound semiconductors is a promising material for high-speed electrical and optoelectronic devices due to its large direct band gap, high electron mobility, high saturation velocity and breakdown voltage which are very important in electronic devices [36,37]. But, due to the large reverse leakage current for metal/n-InP structures it is difficult to obtain a Schottky barrier height (SBH) greater than 0.5 eV [1,37–43]. Thus, the use of n-InP has been hindered in this area. One method for enhancing the Schottky barrier height is to form a tunnel metal–insulator–semiconductor (MIS) structure [44–46]. Another method is to release the surface Fermi level pinning and use a high work function metal [47]. Assuming that the surface Fermi level pinning is caused by high surface state density, passivation technology is needed to reduce the surface states of InP. To fabricate MIS Schottky diodes with an enhanced barrier height, it is useful to develop an *in situ* process in which surface passivation and insulating film deposition are carried out successively.

Efforts have been made to increase the barrier height by growing a high band gap material, such as InAlAs or highly strained InGaP [48,49], as a quasi-insulating layer, or by depositing various dielectric materials on InP [46]. A simpler approach, however, was proposed by Shannon [50] and Wu [51] for Si Schottky contacts. They suggested that the effective Schottky barrier height could be controlled over a certain range (either higher or lower) with a heavily doped surface layer. This concept was proved successfully by Egalsh et al. [52] and Pearton et al. [53] on GaAs by doping the surface p-type with respect to the n-type substrate. A similar structure has been reported on InP by Abid et al. [54], but the reverse leakage current density is extremely large due to poor metallisation contact. However, low BH Schottky diodes of n-InP substrate seem to be a good candidate for the application of zero-bias Schottky detector diodes [40]. In conclusion, we study how pyronine-B organic layer at n-InP/Au interface can affect electrical transport across this interface. Our aim is to study the suitability, thermal stability and possibility of organic-on-inorganic semiconductor contact barrier diode for use in the barrier modification of InP MS diodes. In addition, our purpose is to compare the electrical parameters of the Pyronine-B/semiconductor (n-InP) Schottky diode with those of conventional Au/n-InP Schottky diodes. InP is so thermally unstable that a mild process at low temperatures is necessary to avoid process damage. We also describe the thermal behaviour of Schottky characteristics.

In this study, the current–voltage (*I–V*) and capacitance–voltage (*C–V*) measurements of the gold Schottky contacts on moderately doped n-InP (Au/Pyronine-B/MD n-InP) SBDs were made over the temperature range of 160–400 K. The resultant temperature dependent barrier characteristics of the diodes were interpreted on the basis of the existence of Gaussian distribution of the barrier height.

2. Experimental details

SBDs were fabricated on moderately S-doped n-type InP (1 0 0) substrate with doping concentration of 1.2×10^{16} cm^{-3}. The substrate was sequentially cleaned with trichloroethylene, acetone, methanol and then rinsed in deionised water. The native oxide on the surface was etched in sequence with acid solutions (H_2SO_4:H_2O_2:H_2O = 3:1:1) for 60 s, and (HF (49%):H_2O = 1:1) for another 60 s. After a rinse in deionised water a blow-dry with nitrogen, low resistance Ohmic contact on the back side of the sample was formed by evaporation of Au:Ge eutectic alloy (88% Au:12% Ge) at a pressure of 2.0×10^{-6} mbar, followed by annealing at 300 °C for 5 min in nitrogen atmosphere. Thin film (TF) of Pyronine-B was coated on the clean front surface of the substrate by spinning a solution (7.0 μl of a Pyronine-B solution of 1.0×10^{-6} M in methanol) at 2000 rpm for 5 min. The thickness of the film so obtained was in the range of 10–20 nm across the full substrate surface, and was uniform. *Ex situ* annealing was carried out at 200 °C for 5 min in nitrogen flow for the reaction of the deposited film with the substrate surface. To form the Schottky barriers, finally, circular dots with a diameter of approximately 1 mm of Au were deposited on the substrate by vacuum evaporation technique through a molybdenum mask at $\approx 1.0 \times 10^{-6}$ mbar pressure. Thus, Au/Pyronine-B/MD n-InP Schottky diode was obtained.The current–voltage (*I–V*) measurements of the devices were made using a computer controlled Keithley 487 picoammeter/voltage source and an HP 4192 A LF impedance analyser, respectively over the temperature range of 160–400 K and in dark. The measurements below and above room temperature were performed by mounting the device onto the specially designed cold finger of ARS HC-2 closed-cycle helium cryostat. The device temperature was controlled within an accuracy of ±0.1 K by a Lake Shore 331 model temperature controller.

3. Results and discussion

3.1. The current–voltage characteristics as function of temperature

The molecular structure of the pyronine-B is given in Fig. 1. The pyronine-B is a xanthene-type molecule and has a photophysical fluorescence quantum yield of about 0.56 in alcohols [55]. Since pyronine-B has a conjugation in its structure, it is a good conductive compound. As can be seen from Fig. 1, two electrical structures are possible in which the conjugation is totally different, one where the oxygen assumes a positive charge and in the other possible structure the nitrogen assumes a positive charge. However, because the nitrogen is less electronegative than oxygen, the former can support a positive charge more easily than the latter, and therefore the structure with positive nitrogen is the more likely one [21]. As in the case pyronine-B, the most conducting organic compounds are

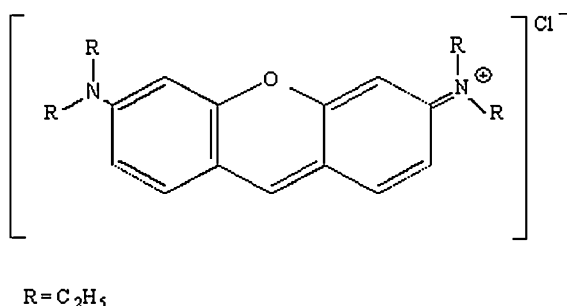

Fig. 1. The molecular structure of the pyronine-B.

of p-type because of the great number of acceptor states that inject holes into the valence band [21] and they have a concentration in the range of 10^{15}–10^{17} cm^{-3}. An important property of organic semiconductors like pyronine-B is that the minimum energy for the formation of a pair of separated free electron and hole is found to be considerably larger than the optical bandgap involving exciton formation.

The current density (J) through a SBD at a forward bias (V), according to thermionic emission (TE) theory, is given by [7]

$$J = J_0 \exp\left(\frac{qV_d}{nkT}\right)\left[1 - \exp\left(-\frac{qV_d}{kT}\right)\right] \quad (1)$$

where $V_d = (V - IR_S)$ is the diode voltage, J_0 is the saturation current density derived from the straight-line intercept of ln(J) at zero-bias and is given by

$$J_0 = A^* T^2 \exp\left(-\frac{q\Phi^j_{b0}}{kT}\right) \quad (2)$$

where q is the electronic charge, V is the definite forward-bias voltage, A^* is the effective Richardson constant, k is the Boltzman constant, T is the absolute temperature, Φ^j_{b0} is the zero-bias barrier height (apparent barrier height) and n is the ideality factor. From Eq. (1), the ideality factor n can be written as

$$n = \frac{q}{kT}\left(\frac{dV}{d\ln(J)}\right) \quad (3)$$

Fig. 2 shows forward bias semi-logarithmic I–V characteristics of the Au/Pyronine-B/MD n-InP Schottky diode in the temperature range of 160–400 K. The values of Φ^j_{b0} and n determined from the intercept and the slopes of the forward bias ln(J) vs. voltage (V) plot according to TE theory are shown in Figs. 3 and 4 as a function of temperature, respectively. Richardson constant of electrons in n-type InP was calculated as $A^* = 120\, m_e^*/m_0 = 9.4\,\mathrm{A\,K^{-2}\,cm^{-2}}$, where m_e^* $(= 0.078m_0)$ is the effective mass for electrons [56]. The experimental values of the apparent barrier height (Φ^j_{b0}) and n range from 0.407 eV and 1.761 at 160 K to 0.756 eV and 1.013 at 400 K, respectively. The low barrier height of metal/n-InP contact has been increased by means of organic layer. The barrier height values of 0.441 eV, 0.46 eV, 0.48 eV and 0.51 eV obtained by Benamara et al. [57], Szydlo and Oliver [58], Ucar et al. [59] and Shi et al. [60], respectively, for Au/n-InP contacts are lower than that of the barrier height (0.664 eV) of the studied diode. This suggests that the organic pyronine-B layer modifies the electrical properties of the n-InP Schottky diode. The studies in literature have shown that effective Schottky barrier could be either increased or decreased by using organic thin layer on inorganic Si semiconductor [61–66]. It is evaluated that the interface properties of the diode is passivated by using organic layer surface to reduce the interaction between metal and inorganic. Indeed, modification of semiconductor surfaces by molecules can lead to the changes in the electronic properties of the metal–semiconductor devices. At study entitled

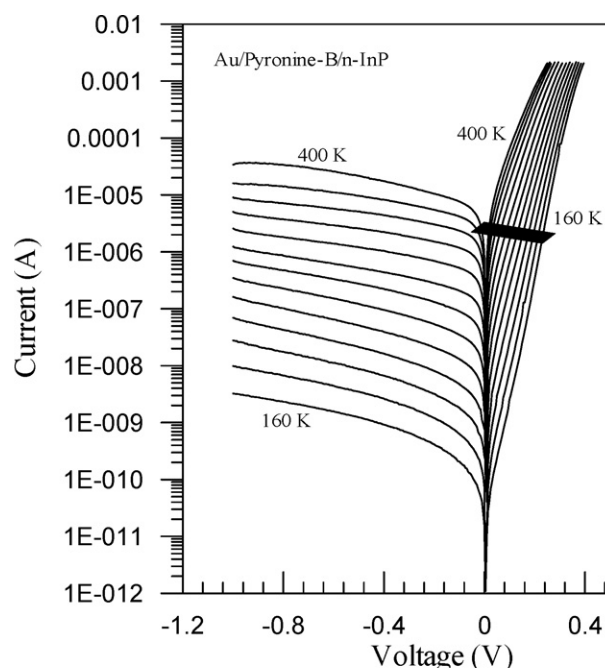

Fig. 2. Semi-log reverse and forward current–voltage characteristics of the Au/Pyronine-B/MD n-InP Schottky barrier diode at various temperatures.

"ultrahigh (100%) barrier modification of n-InP Schottky diode by DNA biopolymer nanofilms", Gullu [67] has demonstrated that DNA biopolymer molecules can control the electrical characteristics of conventional Al/n-InP metal–semiconductor contacts. But, it has been observed that ideality factor n (=1.95) remained remote to ideal limit while barrier height of Al/DNA/n-InP structure increased about 0.44 eV with respect to Al/n-InP in his study, at room temperature. The series resistance R_S varies between 7 and 8 Ω, and is almost independent of temperature. As seen in Figs. 3 and 4, both of the n and Φ^j_{b0} are strongly dependent on temperature and

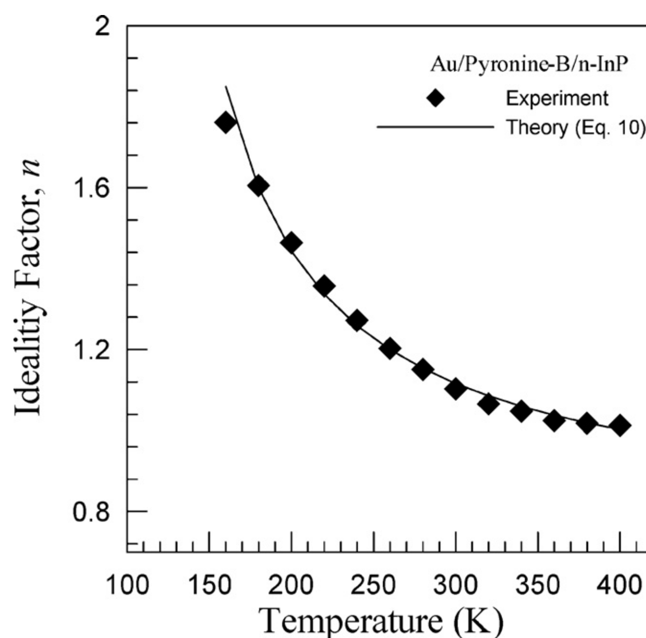

Fig. 3. Temperature dependence of the ideality factor for the Au/Pyronine-B/MD n-InP Schottky barrier diode in the temperature range of 160–400 K. The continuous curve shows the estimated value of the ideality factor using Eq. (10) with $\rho_2 = -0.302$ and $\rho_3 = -0.021$ V.

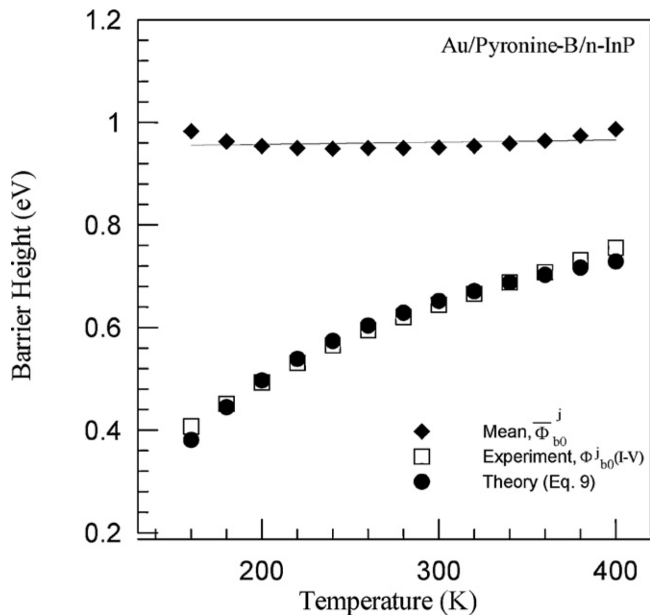

Fig. 4. Temperature dependence of the zero-bias apparent barrier height for the Au/Pyronine-B/MD n-InP Schottky barrier diode in the temperature range of 160–400 K. The closed circles represent the estimated value of Φ_{ap} using Eq. (9) with $\overline{\Phi}_{b0}$ and σ_{s0} are 0.961 eV and 0.1264 eV, respectively.

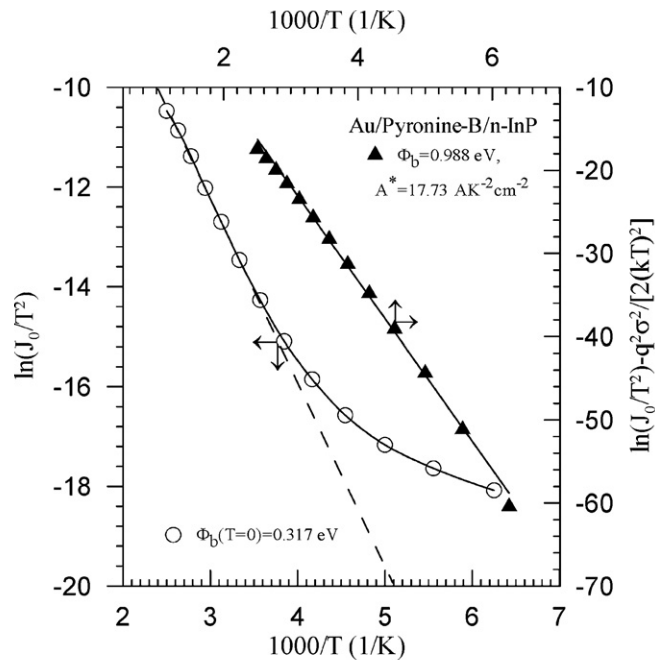

Fig. 5. Richardson plot of the $\ln(J_0/T^2)$ vs. 1000/T and modified Richardson plot, $\ln(J_0/T^2) - (q^2\sigma_{s0}^2/2k^2T^2)$ vs. 1000/T, and its linear fit for the Au/Pyronine-B/MD n-InP Schottky diode according to Gaussian distribution of the barrier heights.

the changes are more pronounced below 260 K. Such a behaviour of the ideality factor has been attributed to the particular distribution of the interface states. Since current transport across the metal–semiconductor interface is controlled by temperature, electrons at low temperature pass over the lower barriers and therefore current will flow through patches of the lower SBH and results in a larger ideality factor. In other words, more electrons have sufficient energy to overcome the higher barrier.

To determine the barrier height in another way, the Richardson plot is drawn. Eq. (2) can be rewritten as

$$\ln\left(\frac{J_0}{T^2}\right) = \ln A^* - \frac{q\Phi^j_{b0}}{kT} \tag{4}$$

Fig. 5 shows the conventional Richardson plot. The experimental data show a bowing at low temperature and it appears a straight line above 260 K. BH obtained from the slope of this straight line yields to be 0.31 eV. Similarly, the value of A^* obtained from the intercept at the ordinate is equal to 3.04×10^{-5} A K^{-2} cm^{-2}, which is lower than the known value of 9.4 A K^{-2} cm^{-2} for n-InP. The bowing in the Richardson plots may be due to the spatial inhomogeneous barrier heights and potential fluctuations at the interface that consist of low and high barrier areas [6,22,23,30]. As will be discussed below, it can be explained by assuming the effects of the image-force, the effect of tunnelling current through the potential barrier, the effect of recombination in the space charge region appearing at low voltage and the variation of the charge distribution near the interface [68].

3.2. The analysis of barrier height inhomogeneities

The ideality factor is simply a manifestation of the barrier uniformity [69]. A significant increase in the ideality factor and decrease in the SBH at low temperature are possibly originated by structural defects in the semiconductor, inhomogeneous doping, interface roughness, interfacial reactions, diffusion/interdiffusion of the contaminations of applied materials on semiconductor surface, inhomogeneities of thickness and composition of the layer, and non-uniformity of interfacial charges or the presence of a thin intentionally grown organic TF layer between the metal and the semiconductor [23,31,70–72]. Since current transport across the MS interface is a temperature-activated process, the current will be controlled by the current through the patches having low BH at the low temperatures. Werner and Güttler [23,31] have proposed an analytical potential fluctuation model for the interpretation of I–V measurements on spatially inhomogeneous PtSi/Si Schottky contacts, while Henisch [73] speculated that the fluctuations in BHs are unavoidable as they exist even in the most carefully processed devices. Furthermore, a linear correlation between the experimental zero-bias BH Φ^j_{b0} and the ideality factor n has been obtained utilizing Tung's pinch-off model [25] by Schmitsdorf et al. [29]. Fig. 6 shows an example of this plot for Au/Pyronine-B/MD n-InP

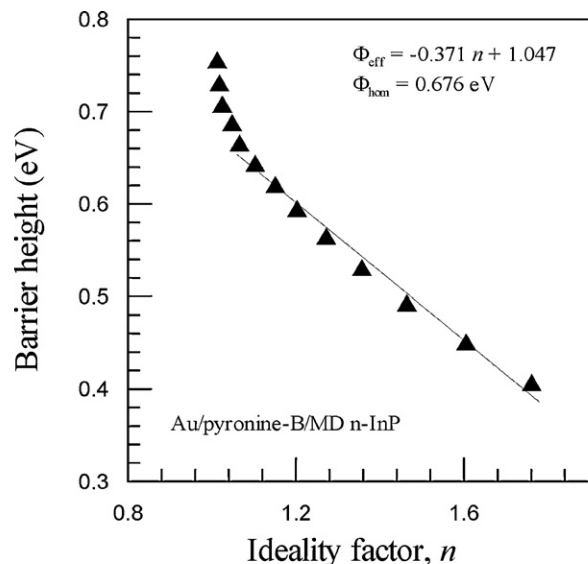

Fig. 6. Plot of the zero-bias BH Φ^j_{b0} vs. ideality factor (n) at the investigated temperature range.

SBD. A linear relationship between the Φ^j_{b0} and n values in Fig. 6 is an indication of the barrier irregularity and can be explained by lateral inhomogeneities of the BHs [29]. A homogeneous BH of approximately 0.676 eV was obtained from the extrapolation of the least-square linear fitting to data to $n = 1$ (Fig. 6).

In order to describe the abnormal behaviours mentioned above, an analytical potential fluctuation model using different types of barrier distribution function at the interface on the spatially inhomogeneous SBDs has been proposed by different workers [6,23,31,69,74–76]. A spatial distribution of the barrier height at the metal–semiconductor interface of Schottky contacts by a Gaussian distribution $P(\Phi^j_b)$ with a standard deviation (σ_s) around a mean SBH ($\overline{\Phi}^j_b$) value has been suggested by Werner and Güttler [23,31] as:

$$P(\Phi^j_b) = \frac{1}{\sigma_s\sqrt{2\pi}}\ \exp\left[-\frac{(\Phi^j_b - \bar{\Phi}^j_b)^2}{2\sigma_s^2}\right] \tag{5}$$

where $1/\sigma_s\sqrt{2\pi}$ is the normalizing constant. Hence, the net current density for any forward bias V is then given by

$$J(V) = A^*T^2 \exp\left[-\frac{q}{kT}\left(\overline{\Phi}^j_b - \frac{q\sigma_s^2}{2kT}\right)\right]\ \exp\left(\frac{qV_d}{kT}\right) \times \left[1 - \exp\left(-\frac{qV_d}{kT}\right)\right] \tag{6}$$

Since the BH is known to depend on the electric field and hence on the applied voltage, the entire profile is also affected by the bias. By assuming a linear bias dependence of both the mean barrier height ($\overline{\Phi}^j_b$) and square of the standard deviation (σ_s^2) with coefficients ρ_2 and ρ_3, (i.e., $\overline{\Phi}^j_b(V) = \overline{\Phi}^j_{b0} + \rho_2 V$ and $\sigma_s^2(V) = \sigma_{s0}^2 + \rho_3 V$), respectively, Eq. (6) gets modified as:

$$J = J_0\ \exp\left(\frac{qV_d}{n_{ap}kT}\right)\left[1 - \exp\left(-\frac{qV_d}{kT}\right)\right] \tag{7}$$

with

$$J_0 = A^*T^2 \exp\left(-\frac{q\Phi_{ap}}{kT}\right) \tag{8}$$

where Φ_{ap} and n_{ap} are apparent barrier height and apparent ideality factor, respectively, and are given by [31]

$$\Phi_{ap} = \bar{\Phi}^j_{b0} - \frac{q\sigma_{s0}^2}{2kT} \tag{9}$$

$$\frac{1}{n_{ap}(T)} - 1 = -\rho_1(T) = -\rho_2 + \frac{q\rho_3}{2kT} \tag{10}$$

where ρ_1, ρ_2 and ρ_3 are the voltage coefficients that may define the voltage deformation of the barrier height distribution, while $\bar{\Phi}^j_{b0}$ and σ_{s0} are the mean barrier height and its standard deviation at the zero-bias ($V = 0$), respectively. Since the Φ_{ap} depends on the distribution parameters $\bar{\Phi}^j_{b0}$ and σ_{s0}, and temperature, the decrease of the apparent zero-bias BH is affected by the existence of the interface inhomogeneities and this effect becomes more significant at low temperatures. On the other hand, the abnormal increase in n_{ap} comes up mainly due to the bias coefficients (ρ_3 and ρ_3) of the mean barrier height and the standard deviation. While ρ_2 gives a constant shift, ρ_3 causes its temperature dependent variation and gets into significance at low temperature.

As Eqs. (2) and (8) are of the same form, the fitting of the experimental J–V data to Eq. (6) gives Φ_{ap} and n_{ap}, which should obey Eqs. (9) and (10). Thus, the plot of Φ_{ap} vs. $q/2kT$ (Fig. 7) should be a straight line yielding $\bar{\Phi}^j_{b0}$ and σ_{s0} from the intercept and slope, respectively. The values of 0.961 eV and 0.126 eV for $\bar{\Phi}^j_{b0}$ and σ_{s0}, respectively were obtained from the least-square linear fitting of the data. Furthermore, as can be seen from Fig. 4, the experimental results of Φ_{ap} (denoted by open squares) fit very well with Eq. (9) (denoted by closed circles), with the same parameters. Also, the correction to the experimental data has been made using Eq. (9). The values of $\bar{\Phi}^j_{b0}$ are marked as zero-bias mean barrier height in Fig. 4. When comparing $\bar{\Phi}^j_{b0}$ and σ_{s0} parameters, it is seen that the standard deviation is ≈13% of the mean zero bias barrier height. The standard deviation is a measure of the barrier homogeneity. The lower value of σ_{s0} corresponds to a more homogeneous barrier height. It is seen that the value of σ_{s0} = 0.126 eV is small compared to the mean value of $\bar{\Phi}^j_{b0} = 0.961$ eV and it indicates larger inhomogeneities at the interface of our Au/Pyronine-B/MD n-InP Schottky structure. But, it is found that is not small compared to the value of σ_{s0} = 0.060 eV for Au/MD n-InP Schottky structure [17]. According to this result, it can be said that interfacial TF (pyronine-B) thickness, inhomogeneities in the composition of the TF layer and non-uniformity of interfacial TF layer charges can cause barrier inhomogeneities. Hence, this inhomogeneity and potential fluctuation dramatically affect low temperature I–V characteristics and it is responsible, in particular, for the curved behaviour in the conventional Richardson plot denoted by open circles in Fig. 5.

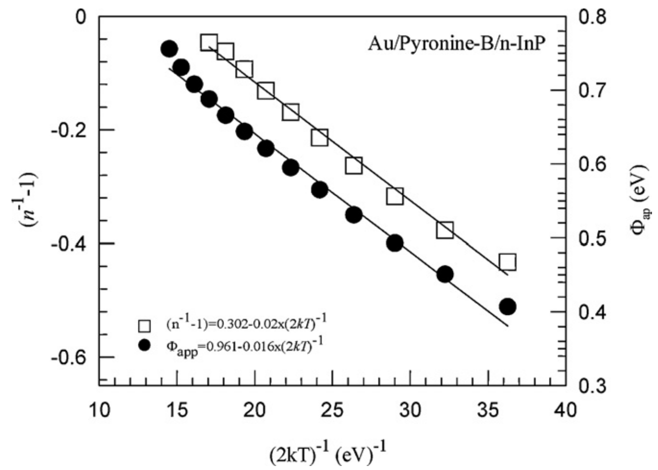

Fig. 7. Zero-bias BH Φ^j_{b0} and $[(1/n_{ap}) - 1]$ vs. $1/(2kT)$ plots and their linear fits for the Au/Pyronine-B/MD n-InP Schottky diode according to Gaussian distribution of the barrier heights.

Fig. 7 also shows the $[(1/n) - 1]$ vs. $1/2kT$ plot. According to Eq. (10), this plot should be a straight line that gives the voltage coefficients ρ_2 and ρ_3 from the intercept and slope, respectively. The values of ρ_2 = −0.302 eV and ρ_3 = −0.021 eV were obtained from this plot. Furthermore, the experimental results of n in Fig. 3 can be seen to fit very well with Eq. (10), denoted by solid line, with the same parameters. The linear behaviour of $[(1/n) - 1]$ vs. $1/2kT$ plot confirms that the ideality factor does indeed denote the voltage deformation of the Gaussian distribution of the BH. It is clear from Eq. (10) that when ρ_3 becomes negative, it will be responsible for the increase in n_{ap} with a decrease in temperature. As ρ_2 becomes also negative, we can conclude that the barrier height and its standard deviation are decreased as bias increases. These results reveal that a bias voltage obviously homogenizes the BH fluctuation, i.e., the higher the bias, the narrower the BH distribution, which can be explained that image forces shift the effective barrier maximum deeper into the semiconductor when the bias voltage increases.

Since the conventional Richardson plot deviates from linearity at low temperatures due to the barrier inhomogeneity, it can be

modified by combining Eqs. (8) and (9) as follows:

$$\ln\left(\frac{J_0}{T^2}\right) - \left(\frac{q^2\sigma_{s0}^2}{2k^2T^2}\right) = \ln A^* - \frac{q\overline{\Phi}_{b0}^j}{kT} \quad (11)$$

Hence, modified Richardson plot $[\ln(J_0/T^2) - (q^2\sigma_{s0}^2/2k^2T^2)$ vs. $1000/T]$ according to Eq. (11) should also be a straight line with the slope and the intercept at the ordinate directly yielding the zero-bias mean barrier height $\bar{\Phi}_{b0}^j$ and A^*, respectively. As can be seen from Fig. 5 (denoted by closed triangles), the modified Richardson plot has a quite good linearity over the whole temperature range corresponding to a single activation energy around $\bar{\Phi}_{b0}^j$. By the least-square linear fitting of the data, $\overline{\Phi}_{b0}^j = 0.977$ eV and $A^* = 17.73\ \mathrm{A\,K^{-2}\,cm^{-2}}$ are obtained. Meanwhile, this value of $\overline{\Phi}_{b0}^j = 0.977$ eV is approximately the same as the value of $\overline{\Phi}_{b0}^j = 0.961$ eV from the plot of Φ_{ap} vs. $1/2kT$ given in Fig. 7, while modified Richardson constant $A^* = 17.73\ \mathrm{A\,K^{-2}\,cm^{-2}}$ is in close agreement with the theoretical value of $A^* = 9.4\ \mathrm{A\,K^{-2}\,cm^{-2}}$. Furthermore, the recreated conventional Richardson plot by using Eqs. (8) and (9) (denoted by solid curve) with the parameters $\overline{\Phi}_{b0}^j = 0.961$ eV, $\sigma_{s0} = 0.040$ eV and $A^* = 17.73\ \mathrm{A\,K^{-2}\,cm^{-2}}$ correlate well with the experimental points denoted by open circles as shown in Fig. 5. These results show that the temperature dependent I–V characteristics of Au/Pyronine-B/MD n-InP Schottky structure obey the Gaussian distribution of BHs as in the case of Al/p-InP [72], Ti/p-InP [77] and Pd/n-InP SBD [78], despite the presence of pyronine-B at the Au/n-InP interface. So, we can speculate that the lateral SB inhomogeneities are not only peculiar to the gold contacts on InP, but also other contact metals.

The decrease in the BH and the increase in the ideality factor with a decrease in the measurement temperature are indicatives of a derivation from the pure TE theory and possibly the TFE mechanism warrants consideration. If current transport is controlled by TFE theory, the connection between the current density and voltage can be expressed by [79]

$$J = J_0 \exp\left(\frac{V}{E_0}\right) \quad (12)$$

$$E_0 = E_{00}\coth\left(\frac{qE_{00}}{kT}\right) \quad (13)$$

$$E_{00} = \frac{q\hbar}{2}\left(\frac{N_d}{m_e^*\varepsilon_s}\right)^{1/2} \quad (14)$$

where E_{00} is the characteristic energy, which is related to the transmission probability, and $\varepsilon_S = 12.4\varepsilon_0$ [56] for InP. The values of E_{00} were evaluated as 2.02 and 1.73 meV for $T = 400$ K and 160 K, respectively. To see the effect of free carriers and to define the dominant current transport mechanism of the Schottky contact, E_{00} values were normalized to kT in the investigated temperature region. As seen in Fig. 8, normalized E_{00}/kT values decreases with temperature and $E_{00} \ll kT$ condition is satisfied for the investigated temperature range. According to the theory, field emission (FE) becomes important when $E_{00} \gg kT$ whereas TFE dominates when $E_{00} \approx kT$ and TE is crucial if $E_{00} \ll kT$. But, the value of kT is equal to 0.0138 eV at 160 K and is slightly greater than E_{00}. Therefore, we can postulate that all over the temperature range TE is the dominant current mechanism. In addition, the ideality factor n is related to the E_{00} as [80]:

$$n_{tun} = \frac{qE_{00}}{kT}\coth\left(\frac{qE_{00}}{kT}\right) \quad (15)$$

According to Eq. (15) the contribution of TFE results only in an increase of 1.033 for n at 160 K. This value is too low to explain our measured value ($n = 1.761$) at 160 K. For other temperatures, the contribution of TFE results only in an increase of 1.051 and 1.150 for n at 300 K and 400 K, respectively. Notice near constacy of n_{tun} over the entire temperature range. This predicts n_{tun} very close to unity for the entire temperature range (160–400 K). Obviously, the tunnelling current is not responsible for the observed barrier lowering and high ideality factor. As a result, the possibility of the FE and TFE can be ruled out. Thus, the higher n values may be related to TE over a Gaussian barrier height distribution.

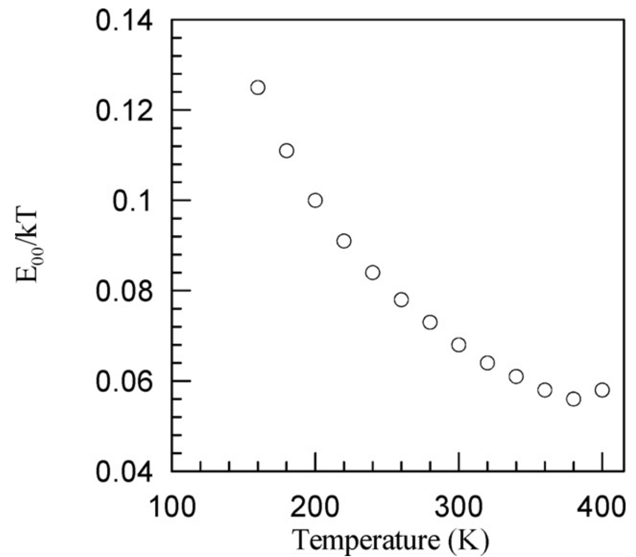

Fig. 8. Normalized E_{00}/kT values as a function of temperature.

Furthermore, using Eq. (15) in our previous study [77], experimental temperature dependent values of the ideality factor obtained from the experimental I–V characteristics in Fig. 2 is in agreement with $E_{00} = 16.0$ meV in the investigated temperature region without considering the bias coefficient of the barrier height, $\beta = 0$. This value of the characteristic energy E_{00} is about eight times larger than the value of 2.02 meV calculated for the n-InP. Such a difference between the theoretical and experimental data is usually obtained and expected for Schottky diodes and this case is connected with local enhancement of electrical field which can also yield a local reduction of the BH [80]. To understand the possible origin of the high characteristic energy, it should be underlined that E_{00} is connected with the transmission probability. Osvald has reported that the ideality factor of inhomogeneous Schottky diodes does not increase for decreasing temperature. He has shown that drift-diffusion current transport approximation is responsible for linear temperature dependency of ideality factor [81].

4. Conclusion

Modification of the interfacial potential barrier for metal/InP diodes has been achieved using a thin interlayer of the pyronine-B organic semiconductor. The higher barrier height value of the device is attributed to the physical barrier properties of pyronine-B layer plus probable native oxide layer between the metal and the inorganic semiconductor. It was observed that ideality factor n (=1.103) remained close to ideal limit while barrier height of Au/Pyronine-B/n-InP structure increased about 0.180 eV with respect to Au/n-InP in the previous study, at room temperature. This is very important for Schottky diodes with interfacial layer. Results reported here propose that the pyronine-B molecule should be considered, among other candidates, as a potential semiconducting non-polymer thin film for the novel MIS devices. The current transport mechanism in Au/Pyronine-B/MD n-InP Schottky barrier diodes has been investigated by means of I–V measurements at various temperatures between 160 and 400 K. It is found that the ideality factor n of the diode decreases while the correspond-

ing zero-bias SBH increasing with an increase in temperature. The significant decrease of zero-bias BH and the increase of the ideality factor at low temperatures cannot be caused by the processes such as tunnelling, generation-recombination currents, image-force lowering, etc. Abnormal behaviour in the temperature dependent ideality factor and the barrier height in the Au/Pyronine-B/MD n-InP SBDs have been successfully cleared up accounting the TE theory with a Gaussian distribution of the BH having spatial variations. The laterally homogeneous SBH and its standard deviation are of 0.961 eV and 0.040 eV, respectively. Also, the mean barrier height and the Richardson constant values have been obtained as 0.977 eV and 17.73 A cm^{-2} K^{-2}, respectively, by means of the modified Richardson plot, $\ln(J_0/T^2) - (q^2\sigma_{s0}^2/2k^2T^2)$ vs. $1000/T$. This value of Richardson constant is in close agreement with the theoretical value of 9.4 A K^{-2} cm^{-2} of electrons in n-type InP. In conclusion, it can be speculated from the diode parameters obtained by I–V techniques that the spatial inhomogeneities of the SBHs is an important factor and could not be ignored in the analysis of temperature dependent electrical characterization of the Schottky structures.

References

[1] M.K. Hudait, P. Venkateswarlu, S.B. Krupanidhi, Solid-State Electron. 45 (2001) 133.
[2] C. Eberspacher, A.L. Fahrenbruch, R.H. Bube, J. Appl. Phys. 58 (1985) 1876.
[3] Ş. Aydogan, K. Cınar, H. Asıl, C. Coskun, A. Turut, J. Alloys Compd. 476 (1-2) (2009) 913.
[4] M. Çakar, Y. Onganer, A. Türüt, Synth. Met. 126 (2002) 213.
[5] F. Yakuphanoglu, J. Phys. Chem. Solids 69 (2008) 949.
[6] F.E. Jones, B.P. Wood, J.A. Myers, C.D. Hafer, M.C. Lonergan, J. Appl. Phys. 86 (1999) 6431.
[7] V. Saxena, B.D. Malhotra, Curr. Appl. Phys. 3 (2003) 293.
[8] R. Singh, D.N. Srivastava, R.A. Singh, Synth. Met. 121 (2001) 1439.
[9] A. Böhler, P. Urbach, J. Schöbel, S. Dirr, H.H. Johannes, S. Wiese, D. Ammermann, W. Kowalsky, Physica E 2 (1998) 562.
[10] Z. Ahmad, H. Muhammad Sayyad, Physica E 41 (2009) 631.
[11] J.F. Wager, C.W. Wilmsen, J. Appl. Phys. 51 (1980) 812.
[12] S.R. Forrest, M.L. Kaplan, P.H. Schmidt, W.L. Feldmann, E. Yanowski, Appl. Phys. Lett. 41 (1992) 90.
[13] S.R. Forrest, M.L. Kaplan, P.H. Schmidt, J. Appl. Phys. 56 (1984) 543.
[14] A.R. Vearey-Roberts, D.A. Evans, Appl. Phys. Lett. 86 (2005) 072105.
[15] Y.J. Liu, H.Z. Yu, Chem. Phys. Chem. 3 (2002) 799.
[16] S. Karatas, M. Cakar, Synth. Met. 159 (2009) 347.
[17] M. Soylu, B. Abay, Microelectron. Eng. 86 (2009) 88.
[18] C. Temirci, M. Çakar, A. Türüt, Y. Onganer, Phys. Stat. Sol. (2004) 3077 (a) no. 14.
[19] T. Clausen, O. Leistiko, Semiconduct. Sci. Technol. 8 (1993) 1731.
[20] P. Urbach, F. Felbier, A. Sörensen, W. Kowalsky, Jpn. J. Appl. Phys. 37 (1998) 1660.
[21] G.D. Sharma, S.K. Gupta, M.S. Roy, Thin Solid Films 333 (1998) 176.
[22] S. Chand, J. Kumar, J. Appl. Phys. 80 (1) (1996) 288.
[23] J.H. Werner, H.H. Güttler, J. Appl. Phys. 73 (3) (1993) 1315.
[24] C.T. Chuang, Solid-State Electron. 27 (1984) 299.
[25] R.T. Tung, Phys. Rev. B 45 (1992) 13502.
[26] F.A. Padovani, in: R.K. Willardson, A.C. Beer (Eds.), Semiconductors and Semimetals, vol. 7A, Academic Press, New York, 1971.
[27] C.R. Crowell, Solid-State Electron. 20 (1977) 171.
[28] R.T. Tung, J.P. Sullivan, F. Schrey, Mater. Sci. Eng. B 14 (1992) 266.
[29] R.F. Schmitsdrof, T.U. Kampen, W. Mönch, J. Vac. Technol. B 15 (1997) 1221.
[30] S.Y. Zhu, R.L. Van Meirhaeghe, C. Detavernier, F. Cordan, G.P. Ru, X.P. Qu, B.Z. Li, Solid-State Electron. 44 (4) (2000) 663.
[31] J.H. Werner, H.H. Gütter, J. Appl. Phys. 69 (3) (1991) 1522.
[32] C.W. Tang, S.A. Van Slyke, Appl. Phys. Lett. 51 (1987) 913.
[33] S. Sohn, K. Kim, S. Kho, D. Jung, J.-h. Boo, J. Alloys Compd. 449 (2008) 191.
[34] H.-H. Huang, S.-Y. Chu, P.-C. Kao, Y.-C. Chen, M.-R. Yang, Z.-L. Tseng, J. Alloys Compd. 479 (2009) 520.
[35] R.H. Friend, R.W. Gymer, A.B. Holmes, J.H. Burroughes, R.N. Marks, C. Taliani, D.D.C. Bradley, D.A. Dos Santos, J.L. Bredas, M. Logdlund, W.R. Salaneck, Nature 397 (1999) 121.
[36] W.-C. Huang, T.-F. Lei, C.-L. Lee, J. Appl. Phys. 78 (1995) 1.
[37] Zs.J. Horwath, V. Rakovics, B. Szentpali, S. Püspöki, Phys. Stat. Sol. C 0 (3) (2003) 916.
[38] P.G. McCafferty, A. Sellai, P. Dawson, H. Elabd, Solid-State Electron. 39 (1996) 583.
[39] N. Newman, T. Kendelwicz, L. Bowman, W.E. Spicer, Appl. Phys. Lett. 46 (1985) 1176.
[40] Zs.J. Horváth, V. Rakovics, B. Szentpáli, S. Püspöki, K. Zydánsky, Vacuum 71 (2003) 113.
[41] L.J. Brillson, C.F. Brucker, A.D. Katnani, N.G. Stoffel, G. Margaritondo, Appl. Phys. Lett. 38 (1981) 784.
[42] E. Hökelek, G.Y. Robinson, J. Appl. Phys. 54 (1983) 5199.
[43] H. Çetin, E. Ayyildiz, Semicond. Sci. Technol. 20 (2005) 625.
[44] R.I. Badran, A. Umar, S. Al-Heniti, A.T. Al-Hajry, T. Al-Harbi, J. Alloys Compd. 508 (2010) 375.
[45] A. Tataroglu, S. Altındal, J. Alloys Compd. 479 (2009) 893.
[46] K. Hattori, Y. Torii, Solid-State Electron. 34 (1991) 527.
[47] T. Sugiuo, Y. Sakamoto, T. Sumiguchi, K. Nomoto, J. Shirafuji, Jpn. J. Appl. Phys. 32 (1993) L1196.
[48] P.Z. Lee, C. Fan, L.G. Meiners, H.H. Wieder, Semicond. Sci. Technol. 5 (1990) 716.
[49] S. Loualiche, A. Ginudi, A. Le Corre, D. Lecrosnier, C. Vaurdy, L. Henry, C. Guillemot, IEEE Electron. Device Lett. 11 (1990) 153.
[50] J.M. Shannon, Solid-State Electron. 19 (1976) 537.
[51] C.Y. Wu, Solid-State Electron. 9 (1981) 857.
[52] S.J. Egalsh, N. Newmen, S. Pan, O. Mo, K. Shenai, W.E. Spicer, F.A. Ponce, M. Collins, J. Appl. Phys. 61 (1987) 5159.
[53] S.I. Pearton, F. Ren, C.R. Abernathy, W.S. Hobson, S.N.G. Chu, J. Kovalchick, Appl. Phys. Lett. 55 (1989) 1342.
[54] Z. Abid, A. Gopinath, F. Williamson, M.I. Nathan, IEEE Electron. Device Lett. 12 (1991) 279.
[55] Y. Onganer, E.L. Quitevis, J. Phys. Chem. 96 (1992) 7996.
[56] A. Neamen Donald, Semiconductor Physics and Devices, Irwin, Boston, 1992; W. Wilmsen, Physics and Chemistry of III–V Compound Semiconductor Interface, Plenum, New York, 1985.
[57] Z. Benamara, B. Akkal, A. Talbi, B. Gruzza, L. Bideux, Mater. Sci. Eng. C 21 (2002) 287.
[58] N. Szydlo, J. Oliver, J Appl. Phys. 50 (1979) 1445.
[59] N. Ucar, A.F. Ozdemir, D.A. Aldemir, S. Cakmak, A. Calik, H. Yildiz, F. Cimilli, Superlattices Microstruct. 47 (2010) 586.
[60] Z.Q. Shi, R. Wallace, W.A. Anderson, Appl. Phys. Lett. 59 (1991) 446.
[61] C. Datavernier, R.L. Van Mairhaeghe, R. Donaton, K. Maex, E. Cardon, J. Appl. Phys. 84 (1998) 3226.
[62] F. Yakuphanoglu, B.-J. Lee, Physica B 390 (1-2) (2007) 151.
[63] M.E. Aydin, F. Yakuphanoglu, J.-H. Eom, D.-H. Hwang, Physica B 387 (1–2) (2007) 239.
[64] M. Cakar, N. Yıldırım, H. Dogan, A. Turut, Appl. Surf. Sci. 252 (6) (2006) 2209.
[65] S. Aydogan, M. Saglam, A. Turut, Polymer 46 (2005) 10982.
[66] S.M. Sze, Physics of Semiconductor Devices, 2nd ed, Wiley, New York, 1981.
[67] O. Gullu, Microelectron. Eng. 87 (2010) 648.
[68] N. Newman, M.V. Schilfgaarde, T. Kendelwicz, M.D. Williams, W.E. Spicer, Phys. Rev. B 33 (1986) 1146.
[69] S. Zhu, R.L. Van Meirhaeghe, S. Forment, G.P. Ru, X.P. Qu, B.Z. Li, Solid-State Electron. 48 (2004) 1205.
[70] J.P. Sullivan, R.T. Tung, M.R. Pinto, W.R. Graham, J Appl. Phys. 70 (1991) 7403.
[71] M.E. Aydin, F. Yakuphanoglu, J. Phys. Chem. Solids 68 (2007) 1770.
[72] Y.P. Song, R.L. Van Meirhaeghe, W.H. Laflare, F. Cardon, Solid-State Electron. 29 (6) (1986) 633.
[73] H.K. Henisch, Semiconductor Contacts, Oxford University, London, 1984, p. 123.
[74] S. Anand, S.B. Carlsson, K. Deppert, L. Montelius, L. Samuelson, J. Vac. Sci. Technol. B 14 (1996) 2794.
[75] Y.G. Chen, M. Ogura, H. Okushi, Appl. Phys. Lett. 82 (2003) 4367.
[76] R.K. Gupta, K. Ghosh, P.K. Kahol, Physica E 42 (2009) 1509.
[77] S. Asubay, Ö. Güllü, B. Abay, A. Türüt, A. Yilmaz, Semicond. Sci. Technol. 23 (2008) 035006.
[78] A. Ashok Kumar, V. Janardhanam, V. Rajagopal Reddy, P. Narasimha Reddy, Superlattices Microstruct. 45 (2009) 22.
[79] E.H. Rhoderick, R.H. Williams, Metal–Semiconductor Contacts, 2nd ed, Oxford, Clarendon, 1988.
[80] Zs.J. Horváth, Solid-State Electron. 39 (1996) 176.
[81] J. Osvald, Microelectron. Eng. 86 (2009) 117.